Abstract #: 983
Program # MI+NS+TuA9

Fabrication and Domain Imaging of Iron Magnetic Nanowire Arrays

D. A. Tulchinsky, M. H. Kelley, J. J. McClelland, R. Gupta, R. J. Celotta

National Institute of Standards and Technology, Gaithersburg, MD 20899

To be published in J. Vac. Sci. Tech. A May/JunA, 1998.

Abstract

Arrays of magnetic nanowires are fabricated by using a corrugated surface, produced by chromium atoms laser-focused in a one-dimensional standing wave, as a shadow mask for an iron evaporator. The deposited iron forms a periodic array consisting of thousands of 20-40 nm high ferromagnetic lines with width of ~100 nm, spaced every 213 nm, and having aspect ratios of 1:1500. Images of the magnetic domain structures of these nanowires are obtained by scanning electron microscopy with polarization analysis (SEMPA). Elongated domains ~100 nm wide and ~16 μm long are observed.

I Introduction

Understanding the magnetic properties of small particles has been a challenge motivated in part by applications to the magnetic recording industry [1,2]. Many questions remain unclear, for instance, the nature of the domain structure of an infinitely long uniform cylinder whose diameter is near the magnetic domain wall thickness, or the role of interparticle interactions in arrays of ferromagnetic magnetic particles [3,4]. In spite of the fundamental and technological interest in 0-D and 1-D magnetic systems, the fabrication and measurement of large uniform arrays of magnetic nanostructures remains a challenge. Current nanofabrication technology

usually involves a tightly focused, highly-spatially-controlled electron beam to expose a resist covered surface [5,6,7] one small area at a time. This is a time consuming process due to the serial nature of the e-beam exposure technique and is normally used to produce one-of-a-kind samples or master photolithography masks. Macroscopic arrays of nanometer scale structures are not normally fabricated with these technologies due to the difficulty in stabilizing the electron beam over the time required to expose each feature. This study presents an inherently parallel, non-lithographic approach to the fabrication of macroscopic, highly uniform arrays of iron nanowires via an evaporation/shadowing technique on a nanoscopically corrugated surface.

II Growth of magnetic nanowire arrays

Corrugated surface fabrication

The magnetic nanowires are fabricated by starting with a corrugated surface produced by laser-focused atomic deposition of Cr atoms [8]. In this technique, chromium atoms emerge from a specially-modified molecular beam epitaxy (MBE) evaporator. For the laser focusing to work, the Cr atoms need to be highly collimated in the direction perpendicular to the axis of the atom beam. Therefore, transverse laser cooling is used to collimate the atomic beam to better than one part in 7000, i.e., 90% of the atoms in the beam are contained within an angular spread of 0.6 mrad. The atom beam is then focused into a pattern by passing it through an optical standing wave formed by reflecting a laser beam from a mirror onto itself as is shown in Fig. 1. The laser wavelength at 425.55 nm corresponds in energy to a near-resonant transition between the Cr $^7S_3$ ground state and the Cr $^7P_4$ excited state. With the laser tuned just off resonance, the Cr atoms are perturbed by a weak dipole force, directed along the gradient of the light intensity. As a result, the laser standing wave acts as a linear array of weak cylindrical lenses, which focus

the Cr atoms into lines. The Cr is deposited onto a substrate positioned immediately beneath the standing wave. The spacing between the nodes of the standing wave is half the laser wavelength or 212.78 nm.

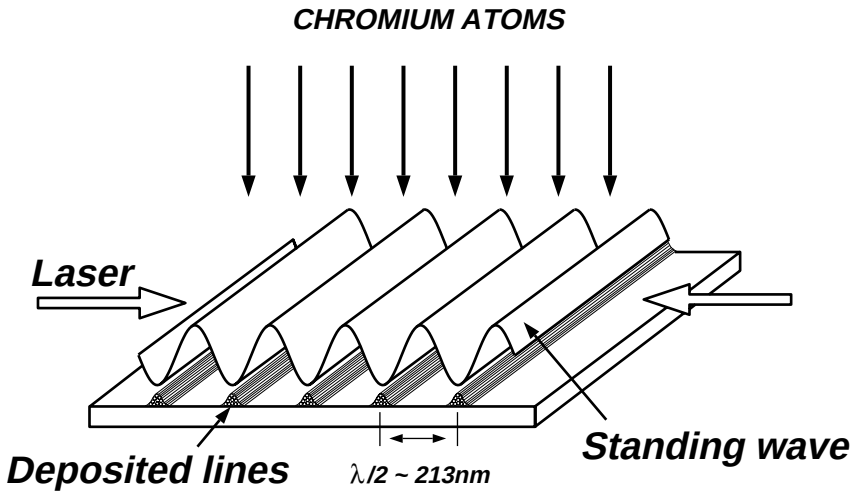

Figure 1 Schematic of laser-focused deposition in a one-dimensional standing wave.

By this technique, a typical sample of Cr lines is grown over an area of up to 1 mm x 0.40 mm [9,10]. Figure 2a shows an atomic force microscope (AFM) topograph of a region of a sample showing a regular array of Cr lines that are highly uniform in both height and width. The height of the lines is primarily a function of the atom beam intensity and the deposition time (~10 min.) The width of the lines is a sensitive function of the atomic beam collimation; the standing-wave intensity and profile; and the wavelength and the spectral width of the laser. The average spacing between the lines, set by the laser wavelength, is considered accurate to at least 0.02%. A better indication of the nanoscopic nature of the Cr lines is seen in the cross sectional transmission electron microscope (TEM) profile of a typical sample as shown in Fig. 2b. The

specific Cr line sample used in this study to form the iron nanowires has Cr line peak heights of ~36 nm with FWHM of ~80 nm as measured by atomic force microscopy (AFM).

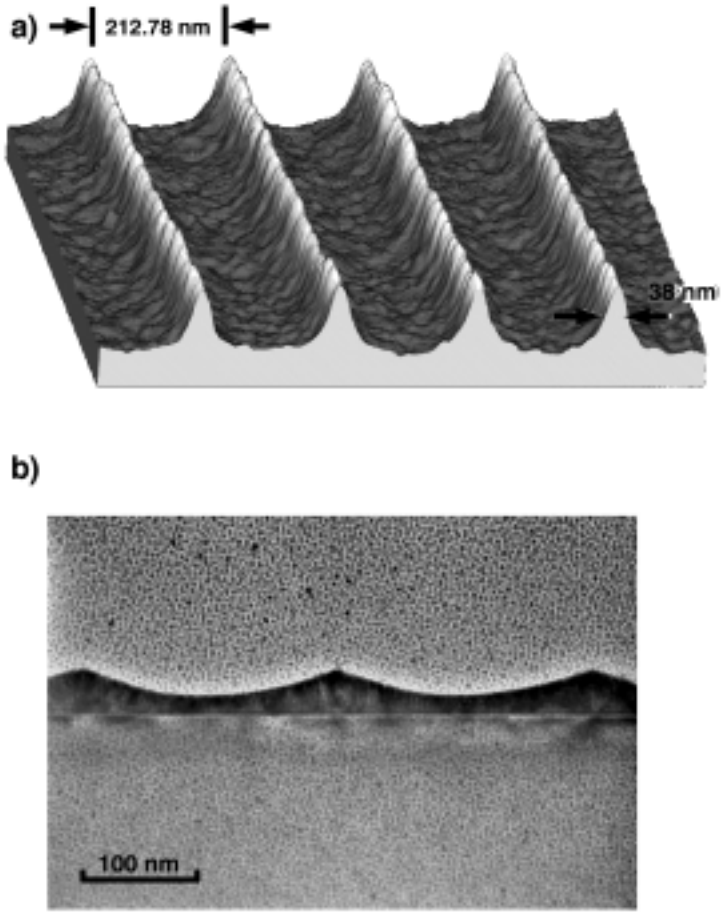

Figure 2(a) Atomic force microscope image of Cr lines formed by laser-focused atomic deposition, showing narrowed linewidth (note this is not the same sample as shown in Fig. 2b). The lines in this image have a height of 8 ± 1 nm (the vertical scale has been expanded to enhance visibility). (b) Transmission electron microscope image of Cr lines formed by laser-focused atomic deposition. Shown is a cross section of the sample described in McClelland et al. (1993), obtained by coating the sample with quartz and sectioning. The lines in this sample are about twice as wide as the sample in Fig. 2a.

Magnetic nanowire production

Once the corrugated Cr surface is produced, the sample is then transferred to a UHV scanning Auger SEMPA microscope. Once the sample surface is cleaned by argon ion sputtering, the magnetic nanowires are fabricated by evaporating iron at a 10^{o} grazing-elevation

onto the sample, perpendicular to the Cr lines as shown in Fig. 3. Iron wires are formed on only one side of the Cr ridges by evaporating 20-40 nm of iron on the leading edge of the Cr lines. Scanning Auger line traces of the resultant Fe/Cr peaks show that distinct Fe/Cr transitions are observed indicating that the shadowing of one Cr peak by the next is sufficient to result in an array of distinct iron wires. The iron lines thus formed are ~100 nm wide and ~0.15 mm long, spaced every 213 nm. These lines have aspect ratios (width:length) of ~ 1:1500 – more than 20 times larger than previously reported [6]. To check the reproducibility of the growth process and the role of the iron thickness on the magnetic structure of the iron lines, multiple sets of iron wires were made on the same Cr line sample – the evaporated iron is easily removed from the Cr line sample by dipping the substrate into a selective iron etch for a few seconds.

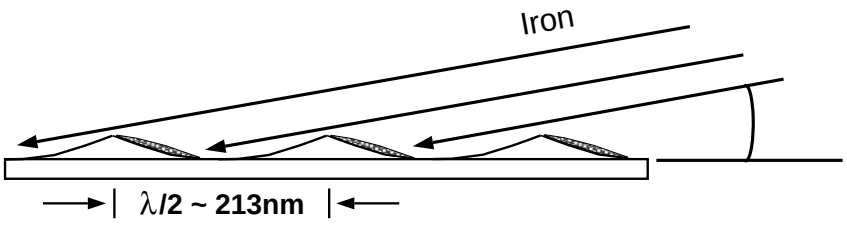

Figure 3 Schematic of the grazing incidence evaporation process used to fabricate the magnetic nanowires.

III Characterization

After iron deposition, the magnetic characteristics of the sample were examined by scanning electron microscopy with polarization analysis (SEMPA) [11,12]. In SEMPA, the secondary electrons collected for imaging also have their spin polarizations measured. The spin polarization (P) of the extracted beam, $P=(N_{\uparrow}-N_{\downarrow})/(N_{\uparrow}+N_{\downarrow})$ (where $N_{\uparrow}(N_{\downarrow})$ are the number of electrons with spins parallel (antiparallel) to a specific magnetization direction), is directly

proportional to the magnetization of the underlying sample. In this way, a SEM equipped with a spin sensitive detector can measure the topography while simultaneously obtaining an image of the sample magnetization/domain patterns.

Figure 4a is a SEMPA image of a 4.5 μm x 5 μm region, clearly resolving the iron lines as distinct domains with magnetizations either "up" (white) or "down" (black). The gray regions between the black and white domains correspond to the nonmagnetic chromium underlayer exposed between the iron lines. The image has roughly three gray levels (1, 0, or –1) as is shown in the line scan across the image, Fig. 4b. This indicates that the magnitude of the magnetization of the sample is nearly up, zero, or down respectively. No magnetization is detected in the

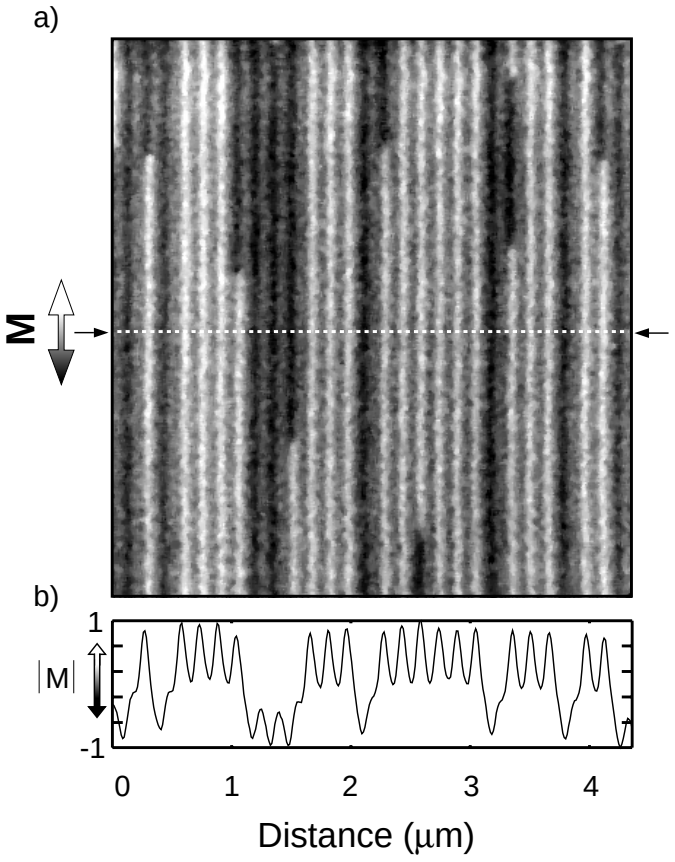

Figure 4 (a) Scanning electron microscopy with polarization analysis (SEMPA) image of the magnetic nanowires formed by evaporating Fe at grazing incidence onto a laser-focused Cr line pattern. (b) Line scan, across Fig. 4a at the arrows, indicating the orientation of the magnetization.

direction transverse to the lines suggesting that the strong shape anisotropy of the lines forces the magnetization of the domains to point in one of two directions along the length axis of the wires.

Determination of the maximum length of a domain is not possible since lower magnification images do not adequately resolve the individual lines. However an estimation of the average length of the as-grown iron domains is possible by counting the number of domain reversals per line in a given image and then applying that to the length of the lines in the image. For Fig. 4a, this means that the average domain length is ~16 μm and the domains have a width to length aspect ratio near 1:160.

A high-resolution close-up image of a domain reversal is shown in Fig. 5. The domain wall appears to form at a ~45^{O} angle to the direction of iron lines. A canted wall is energetically favorable since its magnetostatic energy is less than that required to form a head to head domain wall [13].

For a comparison with the SEMPA images, an attempt was made to use a commercial magnetic force microscope (MFM) to image the magnetic domains. Since a MFM detects the frequency/phase shifts in the resonance of a vibrating cantilever with a magnetic tip, a MFM is sensitive to the local magnetic field gradients on a sample, which in this case occur at the ends of the long axis of each domain. The observed MFM images of the iron line samples were non-reproducible due to the fact that the domain walls were observed to move around on the sample surface as the MFM tip raster scanned the sample. This is not surprising since the remanent field of the MFM tips (~20 mT), required for magnetic sensitivity, is larger than the coercive field of the as-grown Fe wires. A re-examination of the sample by SEMPA, after the MFM imaging, confirmed that the magnetic domain patterns on the sample had been modified from the as-grown state. The post-MFM SEMPA images show domains whose average length is ~750 nm.

The smallest observed domains now have a length of ~200 nm, which is comparable in size to the observed domain wall width for Fe [14].

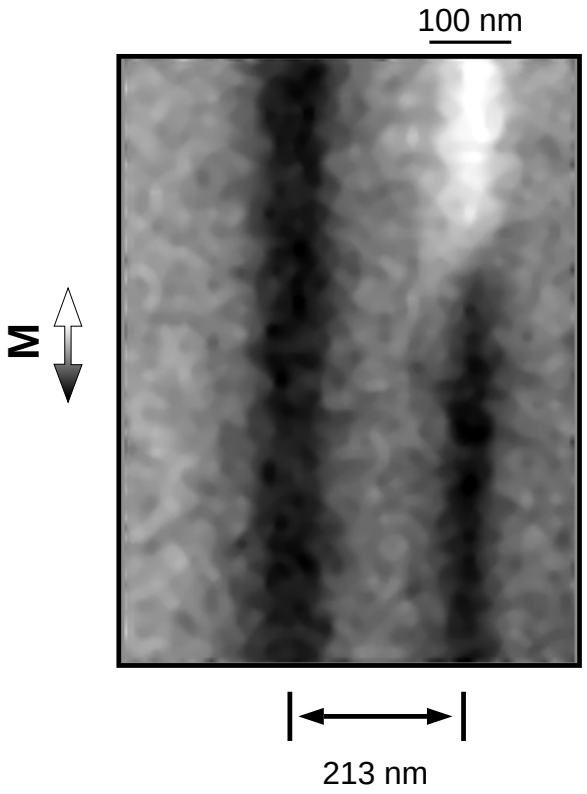

Figure 5 Scanning electron microscopy with polarization analysis (SEMPA) image at high magnification of a domain wall of the sample in Fig. 4a.

IV Conclusions and future prospects

We have described a novel method of using a shadow masking technique to fabricate large scale magnetic nanostructures. The one-dimensional iron wires produced are only one form of nanostructure that might be produced with masks made from laser-focused atomic deposition techniques. Two dimensional masks formed by superimposing two standing waves at 90^{O} across a substrate have already been produced [15] suggesting the possibility of forming 0-D iron islands in a 2-D grid spaced every 213 nm. If used for magnetic recording purposes with

each island recording one bit of information, these dots might have an information density near 16 Gbits/in^2, orders of magnitude above current manufacturing technology.

Acknowledgements

This work partially supported by the Office of Naval Research and by the National Research Council Postdoctoral Research Associateship Program.

Electronic mail: tulch@nist.gov

[1] M. Hehn, *et al.*, Science **272**, 1782 (1996).

[2] K. Hong and N. Giordano, J. Mag. Mag. Mat. **151**, 396 (1995).

[3] A. Aharoni, J. Appl. Phys. **63**, 5879 (1988).

[4] W. F. Brown, Phys. Rev. **105**, 1479 (1957).

[5] A. Maeda, *et al.*, J. Appl. Phys. **76**, 6667 (1994).

[6] M. S. Wei and S. Y. Chou, J. Appl. Phys. **76**, 6680 (1994).

[7] J. Meir, B. Doudin and J-Ph. Ansermet, J. Appl. Phys. **79**, 6010 (1996).

[8] J. J. McClelland, R. E. Scholten, E. C. Palm, R. J. Celotta, Science **262**, 877 (1993).

[9] R. J. Celotta, R. Gupta, R. E. Scholten, J. J. McClelland, J. Appl. Phys. **79**, 6079 (1996).

[10] J. J. McClelland, R. Gupta, Z. J. Jabbour, R. J. Celotta, Aust. J. Phys. **49**, 555 (1996).

[11] M. R. Scheinfein, *et al.*, Rev. Sci. Instum. **60**, 1 (1989).

[12] R. Allenspach, Phys. World **3**, 45 (1994).

[13] R. D. McMichael, private communication.

[14] M. R. Scheinfein, *et al.*, Phys. Rev. B **43**, 3395 (1991).

[15] R. Gupta, J. J. McClelland, Z. J. Jabbour, and R. J. Celotta, Appl. Phys. Lett. **67**, 1378 (1995).